



Synthesis, Biological Evaluation, and Molecular Modeling Studies of New 8-methyl-4-oxo-1,4-dihydroquinoline-3-carbohydrazides as Potential Anti-HIV Agents

Mehrdad Alemi ¹, Fatemeh Kamali ¹, Rouhollah Vahabpour Roudsari ², Zahra Hajimahdi ^{1,*} and Afshin Zarghi ^{1,**}

¹Department of Medicinal Chemistry, School of Pharmacy, Shahid Beheshti University of Medical Sciences, Tehran, Iran

²Medical Lab Technology Department, School of Allied Medical Sciences, Shahid Beheshti University of Medical Sciences, Tehran, Iran

*Corresponding author: Department of Medicinal Chemistry, School of Pharmacy, Shahid Beheshti University of Medical Sciences, Tehran, Iran. Email: z.hajimahdi@sbmu.ac.ir

**Corresponding author: Department of Medicinal Chemistry, School of Pharmacy, Shahid Beheshti University of Medical Sciences, Tehran, Iran. Email: zarghi@sbmu.ac.ir

Received 2022 March 10; Revised 2022 March 31; Accepted 2022 March 31.

Abstract

Background: The development of a highly safe and potent scaffold is a significant challenge in anti-HIV drug discovery.

Objectives: This study aimed at developing a novel series of anti-HIV agents based on HIV integrase inhibitor pharmacophores.

Methods: A novel series of 8-methyl-4-oxo-1,4-dihydroquinoline-3-carbohydrazide derivatives featuring various substituted benzoyl and N-phenyl carboxamide and carbothioamide moieties were designed and synthesized.

Results: According to the biological evaluation, all the developed compounds were effective against HIV at concentrations lower than 150 μ M, associated with no significant cytotoxicity ($CC_{50} > 500 \mu$ M).

Conclusions: Compound 8b, possessing a 4-fluorobenzoyl group, was the most potent compound, with an EC_{50} of 75 μ M. Docking studies revealed that the binding modes of designed compounds are similar to the known HIV integrase inhibitors.

Keywords: Synthesis, 4-oxo-1,4-dihydroquinoline-3-carbohydrazide, HIV Integrase, Molecular Modeling, Anti-HIV

1. Background

Five cases of *Pneumocystis pneumonia* among homosexual males were reported on June 5, 1981, in the Centers for Disease Control's Morbidity and Mortality Weekly Report (1). That study signaled the beginning of the HIV/AIDS epidemic, which has now infected more than 75 million people (2). Acquired immunodeficiency syndrome (AIDS) is the outcome of HIV infection that has not been carefully controlled. Since the epidemic's beginning, 36.3 million people have died from AIDS-related diseases (3-5). Treatment for AIDS is complicated due to the unavailability of vaccines and the presence of viral reservoirs (6, 7). Combination antiretroviral therapy (cART) is the most common treatment for HIV/AIDS (8). The cART has turned HIV-1 infection into a chronic illness with reduced viral load and mortality (9). Drug resistance and pharmacological toxicity are the disadvantages of cART. Therefore, new treatment targets are required (10).

The HIV-1 therapy medicines are commercially available. A combination of two or more active antiretroviral medicines from different classes is advised for the

most effective viral load suppression. Two nucleoside reverse transcriptase inhibitors (NRTIs) plus a third medication, such as an integrase-strand transfer inhibitor (INSTI), non-nucleoside reverse transcriptase inhibitor (NNRTI), or pharmacologically enhanced protease inhibitor (PI), are often used in the first phase of treatment (11). As a result, cART is capable of halting viral replication (12). Human immunodeficiency virus type-1 (HIV-1) and other retroviruses need the retroviral integrase enzyme for replication, which has three structurally different domains: An N-terminal domain, a catalytic core, and a C-terminal domain (13). HIV integrase is an attractive target for therapeutic administration since it lacks a functional human homolog (14). Viral integrase, a 288 amino-acid, 32 kDa enzyme, facilitates the integration of double-stranded viral DNA into the host cell genome (15). The two phases in the integration process are 3'-processing (3'-P) and strand transfer (ST). The first step is the integration of viral DNA into IN in the cytoplasm. In this reaction, IN catalyzes the cleavage of two (or three, depending on in vitro conditions) nucleotides from each of the 3' ends of the DNA (3'-processing) (16, 17). Strand

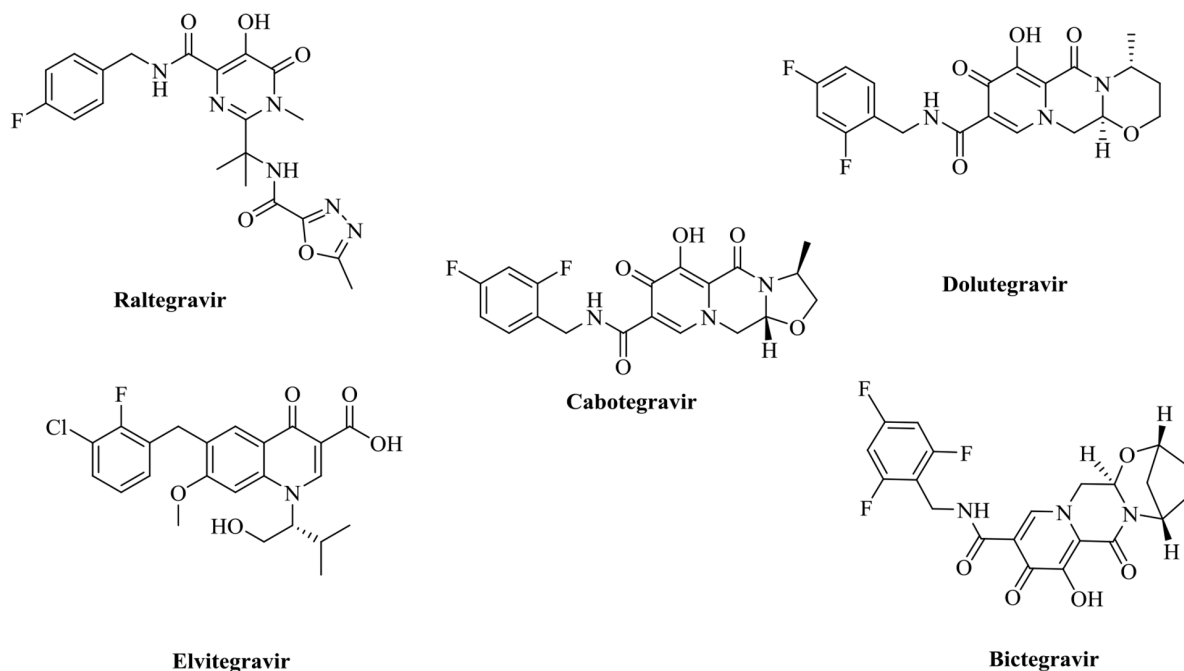


Figure 1. Structure of FDA-approved IN inhibitors

transfer occurs after the preintegration complex (PIC) is transported to the nucleus of infected cells. The viral DNA's 3' hydroxyl group links to the human chromosome during the strand transfer step. The catalytic domain of integrase contains a DDE motif (D64, D116, and E152 amino acids) paired with two Mg^{2+} ions in the enzyme's active site, which are essential for catalytic activity (18, 19). Therefore, metal-based chelation is an approach for inhibiting strand transfer with more selectivity. Elvitegravir, dolutegravir, cabotegravir, and other FDA-approved IN inhibitor pharmacophores (Figure 1) indicate that an INSTI is designed with heteroatoms as a chelating motif and a coplanar hydrophobic aryl group (20-24).

Finding new and safe anti-HIV agents is a top priority since all current inhibitors have been unsatisfactory against HIV strains. The HIV IN inhibitory activity of styrylquinoline and salicylhydrazide aromatics (as seen by structures 1 and 2 in Figure 2) was previously found, but clinical usefulness was limited by their apparent cytotoxicity (25-27). Therefore, a core with minimum toxicity and specific effect is required.

The 4-hydroxyquinoline scaffold found in various structures shows different biological effects, including antibacterial, antioxidant, anti-HIV, anti-fibrosis, antiviral, and anticancer activities (28-31). In addition, our group previously reported some 4-hydroxyquinoline derivatives

possessing promising anti-HIV activity with no significant cytotoxicity (as exemplified by structure 3) (32, 33). This study applied the hybridization technique to obtain a new class of compounds endowed with HIV inhibitory activity and no cytotoxicity. A series of compounds (8a-g) was achieved by merging the 8-methyl-4-hydroxyquinoline group of our previously reported compound 3 with the pharmacophores of the salicylhydrazide (1). In another series of designed compounds (9a-c and 10a-f), we changed the distance between the substituted phenyl moiety and the carbonyl group by one and two atoms, which is critical to achieving the optimal interaction with the IN catalytic site. All of the newly designed compounds were characterized by introducing different substituents in various positions of phenyl rings. To better understand how these compounds block HIV replication, we docked the designed compounds into the HIV integrase protein.

2. Methods

2.1. General

All chemicals and solvents utilized in this study were of the highest quality and obtained from Sigma-Aldrich (Merck KGaA). An Electrothermal-IA9300 melting point device measured the compounds' melting points. A Perkin-

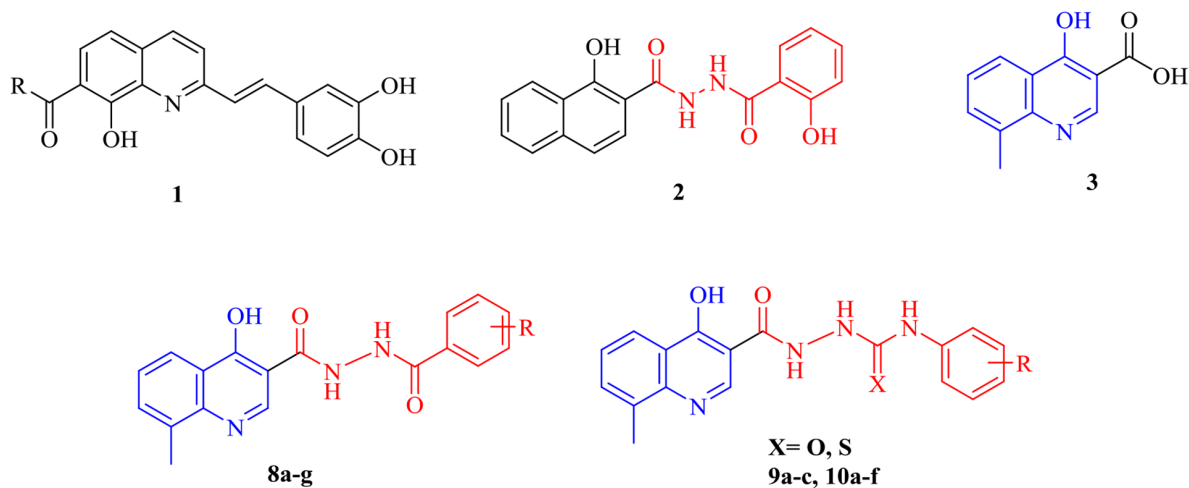


Figure 2. Structure of lead compounds (1, 2, and 3) and our designed structures (8a-g, 9a-c, and 10a-f)

Elmer infrared spectrometer (Model 1420) recorded the infrared spectra. The ^1H and ^{13}C NMR spectra were recorded using tetramethylsilane (TMS) as the internal standard in a Bruker FT-500 MHz NMR spectrometer (500 MHz for ^1H ; 126 MHz for ^{13}C). DMSO- d_6 was the solvent in this operation. Chemical shifts (δ) were measured in parts per million (ppm), and the coupling constant (J) was expressed in hertz (Hz). A 6410 Agilent LCMS device with electrospray ionization (ESI) interface acquired high-resolution mass spectra. A Costech Elemental Combustion System 4010 elemental analyzer analyzed the elements C, H, and N. Microanalysis findings were within 0.4% of theoretical values.

2.2. Synthesis of diethyl 2-((*o*-tolylamino)methylene)malonate (5)

In the first step, a mixture of *ortho*-toluidine (4) (3 mL, 27.9 mmol) and ethoxy Methylene Malonate Diethyl Ester (EMME) (5.6 mL, 28 mmol) was prepared and heated for roughly two hours at 120°C . After completion of the reaction, the mixture was gradually cooled, and the precipitate was washed with *n*-hexane. The obtained product entered the next step after purification.

Yield: 75%; white powder; mp: $61.7 - 62.8^\circ\text{C}$; IR (KBr, spectroscopic grade): 1400 - 1600 (aromatic), 1629, 1670 (C=O), 3273 (N-H) cm^{-1} ; LC-MS (ESI): m/z 300.00 [M+Na] $^+$, 577.10 [2M+Na] $^+$

2.3. Synthesis of ethyl 8-methyl-4-oxo-1,4-dihydroquinoline-3-carboxylate (6)

Compound 5 was dissolved in diphenyl ether, and 2-chlorobenzoic acid was used as the catalyst. Next, the reaction solution was microwave irradiated for two hours at

$> 250^\circ\text{C}$. TLC was used to control the product formation. After the reaction was completed, the resulting mixture was cooled gradually until a precipitate formed, which was then filtered and washed with a large amount of *n*-hexane. The separated solid mass was recrystallized from ethanol.

Yield: 70%; white powder; mp: $266.5 - 267.8^\circ\text{C}$; IR (KBr, spectroscopic grade): 1400 - 1600 (C=C aromatic), 1700 (C=O) cm^{-1} ; LCMS (ESI): m/z 229.8 [M-H] $^-$.

2.4. Synthesis of 8-methyl-4-oxo-1,4-dihydroquinoline-3-carbohydrazide (7)

Compound 6 (2 g, 8.6 mmol) was dissolved in dimethylformamide (DMF) (8 mL), and hydrazine hydrate (4.2 mL, 86.49 mmol) was progressively added. The mixture was stirred at room temperature for 24 hours. After the reaction was completed, the mixture was poured into a container with water and ice and stored at room temperature for four hours. The obtained precipitate was then filtered and washed with a large amount of water. The solid mass was recrystallized from ethanol.

Yield: 80%; white powder; mp: 252°C ; IR (KBr, spectroscopic grade): 1400 - 1600 (C=C aromatic), 1670 (C=O), 3300 (NH) cm^{-1} ; LCMS (ESI): m/z 215.8 [M-H] $^-$.

2.5. General Procedure for the Synthesis of *N'*-[benzoyl] *N'*-8-methyl-4-oxo-1,4-dihydroquinoline-3-carbohydrazide Series (8a-g)

At ambient temperature, a mixture of compound 7 (0.30 g, 1.38 mmol), substituted benzoyl chloride (1.38 mmol), and Na_2CO_3 (0.4 mmol) was prepared in DMF and stirred for 17 hours. After completion of the reaction, the

mixture was slowly poured over crushed ice. The solid was filtered, washed with water, and then recrystallized from ethanol to obtain the final compound.

2.5.1. *N'*-(4-chlorobenzoyl)- 8-methyl- 4-oxo- 1,4-dihydroquinoline- 3-carbohydrazide (8a)

Yield: 50%; white powder; mp: 274 - 275°C; IR (KBr, spectroscopic grade): 1400 - 1600 (aromatic), 1630 (carbonyl), 3276 (N-H) cm^{-1} ; LCMS (ESI): m/z 322.10 [M+H⁺], 344.10 [M+Na⁺]; ¹H NMR (500 MHz, DMSO-d₆): δ ppm 2.53 (s, 3H, CH₃), 7.36-7.39 (t, 1H, benzoyl H₄, J = 7.7 Hz), 7.46-7.49 (t, 2H, benzoyl H₃ & H₅, J = 7.4 Hz), 7.54-7.56 (t, 1H, H₆, J = 7.3 Hz), 7.61 - 7.63 (d, 1H, H₇, J = 7.0 Hz), 7.88 - 7.90 (d, 2H, benzoyl H₂ & H₆, J = 7.3 Hz), 8.14 - 8.15 (d, 1H, H₅, J = 7.9 Hz), 8.61 (s, 1H, H₂), 10.76 (s, 1H, NH), 11.69 (s, 1H, NH), 12.11 (br s, 1H, enolic OH). ¹³C NMR (DMSO-d₆, 126 MHz): δ 17.53, 110.32, 123.88, 125.35, 126.64, 127.90, 128.02, 128.93, 132.28, 132.88, 134.20, 138.12, 143.91, 164.01, 165.29, 176.50; Anal. Calcd. for C₁₈H₁₅N₃O₃: C, 67.28; H, 4.71; N, 13.08. Found: C, 67.37; H, 4.91; N, 13.22.

2.5.2. *N'*-(4-fluorobenzoyl)- 8-methyl- 4-oxo- 1,4-dihydroquinoline- 3-carbohydrazide (8b)

Yield: 44.9%; mp: 291 - 293°C; IR (KBr, spectroscopic grade): 1400 - 1600 (aromatic), 1600,1623 (carbonyl), 3247 (N-H) cm^{-1} ; MS (ESI): m/z 338 [M-H]; ¹H NMR (500 MHz, DMSO-d₆): δ ppm 2.58 (s, 3H, CH₃), 7.35 - 7.38 (t, 2H, 4-fluorobenzoyl H₃ & H₅, J = 8.8 Hz), 7.40 - 7.42 (t, 1H, H₆, J = 7.8 Hz), 7.65 - 7.67 (d, 1H, H₇, J = 7.1 Hz), 7.94 - 8.02 (dd, 2H, 4-fluorobenzoyl H₂ & H₆), 8.17-8.18 (d, 1H, H₅, J = 8.0 Hz), 8.65 (s, 1H, H₂), 10.86 (s, 1H, NH), 11.75 (s, 1H, NH), 12.15 (br s, 1H, enolic OH). ¹³C NMR (DMSO-d₆, 126 MHz): δ 17.52, 110.26, 115.95, 123.87, 125.35, 126.62, 127.91, 129.36, 130.74, 134.20, 138.12, 143.92, 163.41, 164.12, 165.89, 176.49. Anal. Calcd. for C₁₈H₁₄FN₃O₃: C, 63.71; H, 4.16; N, 12.38. Found: C, 63.56; H, 4.27; N, 12.64.

2.5.3. *N'*-(3-fluorobenzoyl)- 8-methyl- 4-oxo- 1,4-dihydroquinoline- 3-carbohydrazide (8c)

Yield: 75%; white powder; mp: 274.4 - 276.9°C; IR (KBr, spectroscopic grade): 1400 - 1600 (aromatic), 1620,1663 (carbonyl), 3280 (N-H) cm^{-1} ; LCMS (ESI): m/z 337.7 [M-H]; ¹H NMR (500 MHz, DMSO-d₆): δ ppm 2.50 (s, 3H, CH₃), 7.31 - 7.37 (dd, 1H, 3-fluorobenzoyl H₄, J = 7.6 Hz), 7.39 - 7.41 (t, 1H, H₆), 7.55-7.57 (m, 1H, 3-fluorobenzoyl H₅), 7.66 - 7.68 (d, 1H, 3-fluorobenzoyl H₂, J = 9.5 Hz), 7.73 - 7.75 (d, 1H, H₇, J = 7.8 Hz), 8.06 - 8.08 (d, 1H, 3-fluorobenzoyl H₆, J = 7.9 Hz), 8.12 - 8.13 (d, 1H, H₅, J = 7.9 Hz), 8.60 (s, 1H, H₂), 10.64 (s, 1H, NH), 11.72 (s, 1H, NH), 12.2 (br s, 1H, enolic OH). ¹³C NMR (DMSO-d₆, 126 MHz): δ 17.52, 110.20, 114.82, 119.24, 123.86, 124.23, 125.37, 126.62, 127.93, 131.20, 134.21, 135.15, 138.13, 143.95, 161.16, 163.59,

165.96, 176.48. Anal. Calcd. for C₁₈H₁₄FN₃O₃: C, 63.71; H, 4.16; N, 12.38. Found: C, 63.49; H, 4.25; N, 12.54.

2.5.4. *N'*-(4-chlorobenzoyl)- 8-methyl- 4-oxo- 1,4-dihydroquinoline- 3-carbohydrazide (8d)

Yield: 39%; white powder; mp: 304 - 305.2°C; IR (KBr, spectroscopic grade): 1400 - 1600 (aromatic), 1637,1665 (carbonyl), 3295 (N-H) cm^{-1} ; LCMS (ESI): m/z 354 [M-H]; ¹H NMR (500 MHz, DMSO-d₆): δ ppm 2.58 (s, 3H, CH₃), 7.42-7.45 (t, 1H, H₆, J = 7.5 Hz), 7.60 - 7.62 (d, 2H, 4-chlorobenzoyl H₃ & H₅, J = 8.5 Hz), 7.67 - 7.68 (d, 1H, H₇, J = 7.0 Hz), 7.94 - 7.96 (d, 2H, 4-chlorobenzoyl H₂ & H₆, J = 8.5 Hz), 8.18 - 8.20 (d, 1H, H₅, J = 7.9 Hz), 8.65 (s, 1H, H₂), 10.93 (s, 1H, NH), 11.77 (s, 1H, NH), 11.80 (br s, 1H, enolic OH). ¹³C NMR (DMSO-d₆, 126 MHz): δ 17.52, 110.24, 123.87, 125.33, 126.61, 127.88, 129.04, 129.95, 131.61, 134.19, 137.12, 138.11, 143.91, 163.93, 164.24, 176.48. Anal. Calcd. for C₁₈H₁₄ClN₃O₃: C, 60.77; H, 3.97; N, 11.81. Found: C, 60.95; H, 3.75; N, 11.61.

2.5.5. 8-Methyl-*N'*-(4-methylbenzoyl)- 4-oxo- 1,4-dihydroquinoline- 3-carbohydrazide (8e)

Yield: 80%; white powder; mp: 260 - 261.4°C; IR (KBr, spectroscopic grade): 1400 - 1600 (aromatic), 1630,1673 (carbonyl), 3298 (N-H) cm^{-1} ; LCMS (ESI): m/z 336.10 [M+H⁺]; ¹H NMR (500 MHz, DMSO-d₆): δ ppm 2.39 (s, 3H, CH₃), 2.58 (s, 3H, CH₃), 7.32 - 7.33 (d, 2H, 4-methylbenzoyl H₃ & H₅, J = 7.9 Hz), 7.41 - 7.44 (t, 1H, H₆, J = 7.6 Hz), 7.66 - 7.68 (d, 1H, H₇, J = 7.1 Hz), 7.83 - 7.84 (d, 2H, 4-methylbenzoyl H₂ & H₆, J = 7.9 Hz), 8.17 - 8.19 (d, 1H, H₅, J = 8.0 Hz), 8.65 (s, 1H, H₂), 10.72 (s, 1H, NH), 11.70 (s, 1H, NH), 12.15 (br s, 1H, enolic OH). ¹³C NMR (DMSO-d₆, 126 MHz): δ 17.52, 21.50, 110.33, 123.86, 125.31, 126.62, 127.89, 128.03, 129.44, 130.06, 134.16, 138.11, 142.26, 143.88, 164.01, 165.19, 176.48. Anal. Calcd. for C₁₉H₁₇N₃O₃: C, 68.05; H, 5.11; N, 12.53. Found: C, 68.25; H, 5.26; N, 12.72.

2.5.6. 8-Methyl-*N'*-(3-methylbenzoyl)- 4-oxo- 1,4-dihydroquinoline- 3-carbohydrazide (8f)

Yield: 50%; white powder; mp: 292 - 293.7°C; IR (KBr, spectroscopic grade): 1400 - 1600 (aromatic), 1650,1670 (carbonyl), 3277,3396 (N-H) cm^{-1} ; LCMS (ESI): m/z 334 [M-H]; ¹H NMR (500 MHz, DMSO-d₆): δ ppm 2.34 (s, 3H, CH₃), 2.53 (s, 3H, CH₃), 7.34 - 7.40 (m, 3H, H₆, 3-methylbenzoyl H₄ & H₅), 7.61 - 7.63 (d, 1H, H₇, J = 7.1 Hz), 7.67 - 7.70 (m, 2H, 3-methylbenzoyl H₂ & H₆), 8.13 - 8.15 (d, 1H, H₅, J = 8.0 Hz), 8.60 (s, 1H, H₂), 10.69 (s, 1H, NH), 11.68 (s, 1H, NH), 12.12 (br s, 1H, enolic OH). ¹³C NMR (DMSO-d₆, 126 MHz): δ 17.53, 21.41, 110.33, 123.89, 125.12, 125.38, 126.65, 127.92, 128.57, 128.81, 132.86, 134.22, 138.14, 138.22, 143.92, 163.93, 165.37, 176.51. Anal. Calcd. for C₁₉H₁₇N₃O₃: C, 68.05; H, 5.11; N, 12.53. Found: C, 68.25; H, 5.29; N, 12.74.

2.5.7. *N'*-(4-methoxybenzoyl)- 8-methyl- 4-oxo- 1,4-dihydroquinoline- 3-carbohydrazide (8g)

Yield: 70%; white powder; mp: 274°C (decomposed); IR (KBr, spectroscopic grade): 1400 - 1600 (aromatic), 1678 (carbonyl), 3276 (N-H) cm^{-1} ; LCMS (ESI): m/z 349.70 [M-H]⁻; ¹H NMR (500 MHz, DMSO-d₆): δ ppm 2.59 (s, 3H, CH₃), 3.84 (s, 3H, OCH₃), 7.05 - 7.06 (d, 2H, 4-methoxybenzoyl H₃' & H₅', J = 8.8 Hz), 7.42 - 7.45 (t, 1H, H₆, J = 7.5 Hz), 7.67 - 7.68 (d, 1H, H₇, J = 7.1 Hz), 7.91 - 7.93 (d, 2H, 4-methoxybenzoyl H₂' & H₆', J = 8.7 Hz), 8.18 - 8.20 (d, 1H, H₅, J = 7.9 Hz), 8.65 (s, 1H, H₂), 10.65 (s, 1H, NH), 11.68 (s, 1H, NH), 12.16 (br s, 1H, enolic OH). ¹³C NMR (DMSO-d₆, 126 MHz): δ 17.52, 55.85, 110.38, 114.14, 123.88, 124.98, 125.33, 126.64, 127.89, 129.90, 134.18, 138.12, 143.88, 162.45, 164.04, 164.81, 176.50. Anal. Calcd. for C₁₉H₁₇N₃O₄: C, 64.95; H, 4.88; N, 11.96. Found: C, 64.75; H, 5.02; N, 11.81.

2.6. General Procedure for the Synthesis of *N*-(phenyl)- 2-(8-methyl- 4-oxo- 1,4-dihydroquinoline- 3-carbonyl) hydrazine- 1-carboxamide Series (9a-c)

Compound 7 (0.22 g, 0.1 mmol) was dissolved in dry DMF (4 mL). Then, isocyanate derivatives (0.1 mmol) were progressively added to the mixture. The reaction solution was stirred for 24 hours at room temperature. Thin-layer chromatography was used to monitor and control the product. Water and ice were poured into the reaction to form a precipitate, which was then filtered through a Buchner funnel and thoroughly rinsed with plenty of water. The precipitate was crystallized using 96% ethanol solution.

2.6.1. 2-(8-Methyl- 4-oxo- 1,4-dihydroquinoline- 3-carbonyl)- *N*-phenylhydrazine- 1-carboxamide (9a)

Yield: 73%; white powder; mp: 310.9°C (decomposed); IR (KBr, spectroscopic grade): 1400 - 1600 (aromatic), 1641,1676 (C=O), 2589 - 3500 (OH), 3338, 3462 (NH) cm^{-1} ; LCMS (ESI): m/z 337.0 [M+H]⁺; ¹H NMR (500 MHz, DMSO-d₆): δ ppm 2.57 (s, 3H, CH₃), 6.94 - 6.98 (t, 1H, *N*-phenyl H₄', J = 8.0 Hz), 7.24 - 7.28 (t, 2H, *N*-phenyl H₃' & H₅', J = 8.0 Hz), 7.40 - 7.44 (t, 1H, H₆, J = 8.0 Hz), 7.47 (d, 2H, *N*-phenyl H₂' & H₆', J = 8.0 Hz), 7.65 (d, 1H, H₇, J = 4.0 Hz), 8.17 (d, 1H, H₅, J = 8.0 Hz), 8.45 (br s, 1H, NH), 8.61 (s, 1H, H₂), 8.92 (s, 1H, NH), 11.41 (br s, 1H, NH), 12.14 (br s, 1H, enolic OH); ¹³C NMR (DMSO-d₆, 126 MHz): δ 17.51, 110.45, 118.79, 122.32, 123.88, 125.30, 126.69, 127.86, 129.14, 134.16, 138.12, 140.12, 143.78, 155.34, 164.45, 176.44; Anal. Calcd. for C₁₈H₁₆N₄O₃: C, 64.28; H, 4.79; N, 16.66. Found: C, 64.42; H, 4.66; N, 16.85.

2.6.2. *N*-benzyl- 2-(8-methyl- 4-oxo- 1,4-dihydroquinoline- 3-carbonyl) hydrazine- 1-carboxamide (9b)

Yield: 70%; white powder; mp: 280.1°C (decomposed); IR (KBr, spectroscopic grade): 1400 - 1600 (aromatic), 1653

(C=O), 2783 - 3429 (OH), 3310 (NH) cm^{-1} ; LCMS (ESI): m/z 351 [M+H]⁺, 372.9 [M+Na]⁺; ¹H NMR (500 MHz, DMSO-d₆): δ ppm 2.56 (s, 3H, CH₃), 4.25 (d, 2H, -CH₂, J = 4.0 Hz), 7.07 (br s, 1H, NH), 7.21 - 7.24 (t, 1H, *N*-benzyl H₄', J = 8.0 Hz), 7.27 - 7.34 (m, 4H, *N*-benzyl H₂', H₃', H₅' & H₆'), 7.38-7.42 (t, 1H, H₆, J = 8.0 Hz), 7.65 (d, 1H, H₇, J = 8.0 Hz), 8.15 (d, 1H, H₅, J = 8.0 Hz), 8.22 (br s, 1H, NH), 8.61 (s, 1H, H₂), 11.26 (br s, 1H, NH), 12.12 (br s, 1H, enolic OH); ¹³C NMR (DMSO-d₆, 126 MHz): δ 17.51, 110.65, 123.88, 125.25, 126.69, 127.02, 127.44, 127.81, 128.62, 134.12, 138.09, 140.99, 143.73, 158.38, 164.72, 176.43; Anal. Calcd. for C₁₉H₁₈N₄O₃: C, 65.13; H, 5.18; N, 15.99. Found: C, 65.25; H, 5.33; N, 15.78.

2.6.3. *N*-(3,4-dichlorophenyl)- 2-(8-methyl- 4-oxo- 1,4-dihydroquinoline- 3-carbonyl) hydrazine- 1-carboxamide (9c)

Yield: 62%; white powder; mp: 292.4°C (decomposed); IR (KBr, spectroscopic grade): 1400 - 1600 (aromatic), 1648, 1686 (C=O), 2587 - 3500 (OH), 3335, 3488 (NH) cm^{-1} ; LCMS (ESI): m/z 405.0 [M+H]⁺; ¹H NMR (500 MHz, DMSO-d₆): δ ppm 2.57 (s, 3H, CH₃), 7.40 - 7.44 (t, 2H, H₆, J = 8.0 Hz), 7.49 - 7.50 (d, 1H, 3,4-dichlorophenyl H₆', J = 8.0 Hz), 7.65 - 7.67 (d, 1H, H₇, J = 8.0 Hz), 7.87 (d, 1H, 3,4-dichlorophenyl H₅', J = 8.0 Hz), 8.17 (d, 1H, H₅, J = 8.0 Hz), 8.61 (s, 1H, H₂), 8.64 (s, 1H, 3,4-dichlorophenyl H₂'), 9.24 (s, 1H, NH), 11.38 (br s, 1H, NH), 12.16 (br s, 1H, enolic OH); ¹³C NMR (DMSO-d₆, 126 MHz): δ 17.52, 110.43, 118.97, 119.99, 123.57, 123.88, 125.36, 126.70, 127.89, 130.92, 131.31, 134.21, 138.12, 140.49, 143.86, 176.46; Anal. Calcd. for C₁₈H₁₄Cl₂N₄O₃: C, 53.35; H, 3.48; N, 13.83. Found: C, 53.52; H, 3.59; N, 13.99.

2.7. General Procedure for the Synthesis of 2-(8-dimethyl- 4-oxo- 1,4-dihydroquinoline- 3-carbonyl)- *N*-phenylhydrazine- 1-carbothioamide (10a-f)

Compound 7 (0.22 g, 0.1 mmol) was dissolved in dry DMF (4 mL). Next, isothiocyanate derivatives (0.1 mmol) were progressively added to the mixture. The reaction solution was stirred for 4 hours at room temperature. Thin-layer chromatography was used to monitor and control the product. Water and ice were poured into the reaction to form a precipitate, which was then filtered through a Buchner funnel and thoroughly rinsed with plenty of water. The precipitate was crystallized using 96% ethanol solution.

2.7.1. 2-(8-Methyl- 4-oxo- 1,4-dihydroquinoline- 3-carbonyl)- *N*-phenylhydrazine- 1-carbothioamide (10a)

Yield: 80%; white powder; mp: 237.6°C (decomposed); IR (KBr, spectroscopic grade): 1400 - 1600 (aromatic), 1646,1662 (C=O), 2765 - 3392 (OH), 3224, 3324 (NH) cm^{-1} ; LCMS (ESI): m/z 374.8 [M+Na]⁺, 353.0 [M+H]⁺; ¹H NMR (500

MHz, DMSO- d_6): δ ppm 2.58 (s, 3H, CH₃), 7.12 - 7.16 (t, 1H, N-phenyl H₄, J = 8.0 Hz), 7.31 - 7.35 (t, 2H, N-phenyl H₃ & H₅, J = 8.0 Hz), 7.40 - 7.44 (t, 1H, H₆, J = 8.0 Hz), 7.53 (m, 2H, N-phenyl H₂ & H₆'), 7.66 (d, 1H, H₇, J = 8.0 Hz), 8.18 (d, 1H, H₅, J = 8.0 Hz), 8.62 (s, 1H, H₂), 9.87 (br s, 2H, NH), 12.16 (br s, 1H, enolic OH), ¹³C NMR (DMSO- d_6 , 126 MHz): δ 17.52, 123.89, 125.36, 126.64, 127.87, 128.72, 134.22, 138.10, 139.73, 143.71, 176.33; Anal. Calcd. for C₁₈H₁₆N₄O₂S: C, 61.35; H, 4.58; N, 15.90. Found: C, 61.42; H, 4.80; N, 15.70.

2.7.2. 2-(8-Methyl- 4-oxo- 1,4-dihydroquinoline- 3-carbonyl)- N-(o-tolyl) hydrazine- 1-carbothioamide (10b)

Yield: 81%; white powder; mp: 237.1°C (decomposed); IR (KBr, spectroscopic grade): 1400 - 1600 (aromatic), 1648, 1670 (C=O), 2878 - 3400 (OH), 3130, 3290 (NH) cm⁻¹; LCMS (ESI): m/z 367.0 [M+H⁺]; ¹H NMR (500 MHz, DMSO- d_6): δ ppm 2.21 (s, 3H, CH₃), 2.57 (s, 3H, 8-CH₃), 7.13 - 7.22 (m, 4H, N-o-tolyl H₃, H₄, H₅ & H₆'), 7.40 - 7.44 (t, 1H, H₆, J = 8.0 Hz), 7.66 (d, 1H, H₇, J = 8.0 Hz), 8.17 (d, 1H, H₅, J = 8.0 Hz), 8.62 (s, 1H, H₂), 9.53 (br s, 1H, NH), 9.72 (br s, 1H, NH), 11.49 (br s, 1H, NH), 12.15 (br s, 1H, enolic OH), ¹³C NMR (DMSO- d_6 , 126 MHz): δ 17.53, 18.18, 123.89, 125.33, 126.64, 126.88, 127.85, 130.57, 134.20, 138.09, 143.67, 158.38, 164.72, 176.43; Anal. Calcd. for C₁₉H₁₈N₄O₂S: C, 62.28; H, 4.95; N, 15.29. Found: C, 62.36; H, 4.85; N, 15.39.

2.7.3. 2-(8-Methyl- 4-oxo- 1,4-dihydroquinoline- 3-carbonyl)- N-(m-tolyl) hydrazine- 1-carbothioamide (10c)

Yield: 75.6%; white powder; mp: 212.6°C; IR (KBr, spectroscopic grade): 1400 - 1600 (aromatic), 1668 (C=O), 2759 - 3500 (OH), 3230, 3330 (NH) cm⁻¹; LCMS (ESI): m/z 367 [M+H⁺]; ¹H NMR (500 MHz, DMSO- d_6): δ ppm 2.29 (s, 3H, CH₃), 2.58 (s, 3H, 8-CH₃), 6.95 (d, 1H, m-tolyl H₄, J = 8.0 Hz), 7.19 - 7.23 (t, 1H, m-tolyl H₅, J = 8.0 Hz), 7.34 (m, 2H, m-tolyl H₂ & H₆'), 7.40 - 7.44 (t, 1H, H₆, J = 8.0 Hz), 7.66 (d, 1H, H₇, J = 8.0 Hz), 8.18 (d, 1H, H₅, J = 8.0 Hz), 8.62 (s, 1H, H₂), 9.80 (br s, 2H, NH), 12.16 (d, 1H, enolic OH), ¹³C NMR (DMSO- d_6 , 126 MHz): δ 17.53, 21.47, 123.89, 125.36, 126.64, 127.87, 134.22, 138.09, 139.59, 143.70, 176.32; Anal. Calcd. for C₁₉H₁₈N₄O₂S: C, 62.28; H, 4.95; N, 15.29. Found: C, 62.39; H, 5.12; N, 15.39.

2.7.4. 2-(8-Methyl- 4-oxo- 1,4-dihydroquinoline- 3-carbonyl)- N-(p-tolyl) hydrazine- 1-carbothioamide (10d)

Yield: 85.6%; white powder; mp: 232.4°C (decomposed); IR (KBr, spectroscopic grade): 1400 - 1600 (aromatic), 1615, 1639 (C=O), 2757 - 3379 (OH), 3210, 3250 (NH) cm⁻¹; LCMS (ESI): m/z 367 [M+H⁺]; ¹H NMR (500 MHz, DMSO- d_6): δ ppm 2.28 (s, 3H, CH₃), 2.57 (s, 3H, 8-CH₃), 7.13 (d, 2H, p-tolyl H₃ & H₅, J = 8.0 Hz), 7.38 - 7.44 (m, 3H, H₆ and p-tolyl H₂ & H₆'), 7.66 (d, 1H, H₇, J = 8.0 Hz), 8.17 (d, 1H, H₅, J = 8.0 Hz), 8.61 (s, 1H, H₂), 9.79 (br s, 2H, NH), 12.15 (br s, 1H, enolic OH), ¹³C NMR (DMSO- d_6 , 126 MHz): δ 17.52, 21.00, 123.89, 125.35,

126.64, 127.86, 129.17, 134.21, 137.11, 138.09, 143.69, 176.33; Anal. Calcd. for C₁₉H₁₈N₄O₂S: C, 62.28; H, 4.95; N, 15.29. Found: C, 62.35; H, 4.73; N, 15.09.

2.7.5. 2-(8-Methyl- 4-oxo- 1,4-dihydroquinoline- 3-carbonyl)- N-(4-fluorophenyl) hydrazine- 1-carbothioamide (10e)

Yield: 81%; white powder; mp: 239.7°C (decomposed); IR (KBr, spectroscopic grade): 1400 - 1600 (aromatic), 1647, 1662 (C=O), 2789 - 3500 (OH), 3218 (NH) cm⁻¹; LCMS (ESI): m/z 370.8 [M+H⁺]; ¹H NMR (500 MHz, DMSO- d_6): δ ppm 2.58 (s, 3H, CH₃), 7.14 - 7.19 (t, 2H, 4-fluorophenyl H₃ & H₅, J_{H,F} = 12.0 Hz), 7.40 - 7.44 (t, 1H, H₆, J = 8.0 Hz), 7.49 (m, 2H, 4-fluorophenyl H₂ & H₆'), 7.66 (d, 1H, H₇, J = 8.0 Hz), 8.17 (d, 1H, H₅, J = 8.0 Hz), 8.62 (s, 1H, H₂), 9.85 (br s, 2H, NH), 12.17 (br s, 1H, enolic OH), ¹³C NMR (DMSO- d_6 , 126 MHz): δ 17.53, 115.36, 123.89, 125.39, 126.64, 127.89, 134.24, 136.05, 138.10, 143.75, 176.35. Anal. Calcd. for C₁₈H₁₅FN₄O₂S: C, 58.37; H, 4.08; N, 15.13. Found: C, 58.55; H, 4.22; N, 15.28.

2.7.6. N-(4-methoxyphenyl)- 2-(8-methyl- 4-oxo- 1,4-dihydroquinoline- 3-carbonyl) hydrazine- 1-carbothioamide (10f)

Yield: 70.2%; white powder; mp: 230.7 - 233.3°C (decomposed); IR (KBr, spectroscopic grade): 1400 - 1600 (aromatic), 1648 (C=O), 2795 - 3395 (OH), 3259 (NH) cm⁻¹; LCMS (ESI): m/z 383.1 [M+H⁺]; ¹H NMR (500 MHz, DMSO- d_6): δ ppm 2.57 (s, 3H, CH₃), 3.74 (s, 3H, OCH₃), 6.90 (d, 2H, 4-methoxyphenyl H₃ & H₅, J = 8.0 Hz), 7.35 (d, 2H, 4-methoxyphenyl H₂ & H₆'), 7.40-7.44 (t, 1H, H₆, J = 8.0 Hz), 7.66 (d, 1H, H₇, J = 8.0 Hz), 8.17 (d, 1H, H₅, J = 8.0 Hz), 8.61 (s, 1H, H₂), 9.72 (br s, 2H, NH), 12.14 (br s, 1H, enolic OH); Anal. Calcd. for C₁₉H₁₈N₄O₃S: C, 59.67; H, 4.74; N, 14.65. Found: C, 59.53; H, 4.66; N, 14.38.

2.8. Molecular Docking Study

The docking study was performed using the high-resolution X-ray diffraction structure of the Prototype Foamy Virus (PFV) crystal (PDB code: 3OYA) in association with Mg⁺² and raltegravir. To prepare the ligand and perform conformational analysis, we utilized HyperChem 8.0.10. Protein and ligands were prepared using Autodock tools 1.5.6 (ADT) from the molecular graphics laboratory (MGL) Tools (34). In this simulation, water molecules were removed to simplify calculations. The co-crystallized ligand was extracted, Kollman united partial charges were added, and non-polar hydrogens were merged. The active site was defined as a grid box with dimensions of 20 × 20 × 20 Å enclosing the crystallographic ligand raltegravir. The docking used in this study is a semi-flexible method of operation. AutoDock4 software was used to insert ligands in the enzyme's binding site.

2.9. In Vitro Anti-HIV-1 and Cytotoxicity Assay Method

The synthesized compounds were evaluated for anti-HIV activity by single-cycle replication assay as reported previously. As part of this study, an HIV-1 genome-mutated in the poly (pol) gene was co-transfected with plasmids that expressed reverse transcriptase (RT) and integrase (IN), as well as glycoprotein G of the vesicular stomatitis virus (VSV). The virions produced in HEK 293 T cells were antigenic but only replicated for one cycle (first-generation single-cycle replicable (SCR) virions). DMSO was used to dissolve the compounds at concentrations ranging from 10 mmol/L to 10 μ mol/L. These stocks were diluted 100 times in the cell environment, resulting in final compound concentrations ranging from 100 μ mol/L to 10 nmol/L. We used zidovudine (AZT) and DMSO (1% v/v) as positive and negative controls in the experiment, respectively. All tests were run three times. HeLa cells (6×10^3 per well of 96-well plates) were infected with single-cycle replicable HIVNL4-3 virions (200 ng p24) in the presence of various concentrations of compounds. Compounds were added to the cell environment simultaneously with a viral infection. Capture ELISA (Biomerieux, France) measured the p24 antigen load in cell culture supernatant 72 hours after infection. The inhibition rate of p24 (%) was used to compute the percentage inhibition of p24 expression in the treated culture. The XTT proliferation technique was used to evaluate the cellular toxicity of substances. The XTT (sodium 3-[1 (phenyl aminocarbonyl)-3,4-tetrazolium]-bis(4-methoxy-6-nitro) benzene sulfonic acid) reagent was used according to the kit instruction (Roche, Germany). In a CO₂ incubator, cells were cultured in 96-well plates (3,5104 cells/well) with fresh phenol-red free medium and incubated for 72 hours. Next, 50 μ L of XTT was added to each well and incubated for four hours at 37°C. Plates were evaluated by an ELISA reader at the test and reference OD of 450 and 630 nm, respectively. The cytotoxic concentration that reduced the number of viable cells by 50% (CC₅₀) was calculated after determining the p24 load in HIV-1 replication assay plates (35-38).

3. Results and Discussion

3.1. Chemistry

The synthesis of the target compounds is described in Figure 3. O-toluidine (4) was used to begin the synthesis of the target compounds. Compound 5 (diethyl 2-((o-tolylamino) malonate) was synthesized by condensing o-toluidine with EMME. Compound 5 was turned into ethyl 8-methyl-4-oxo-1,4-dihydroquinoline-3-carboxylate (6) in diphenyl ether containing catalytic 2-chlorobenzoic acid. A DMF solution of hydrazine was used to make

8-methyl-4-oxo-1,4-dihydroquinoline-3-carbohydrazide (compound 7) from compound 6. Compound 7 was the primary intermediate for synthesizing three series of substances. Compound 7 interacted with substituted benzoyl chlorides in DMF with a catalytic quantity of Na₂CO₃ to produce N'-[substituted benzoyl] N'-8-methyl-4-oxo-1,4-dihydroquinoline-3-carbohydrazide derivatives (8a-g). The second and third series of compounds were prepared by the reaction of compound 7 with the phenyl isocyanate and phenyl isothiocyanate derivatives in dry DMF to produce compounds 9a-c and 10a-f, respectively. The structure of synthesized compounds was determined by ¹H-NMR, ¹³C-NMR, LC-MS technique, and elemental analysis.

3.2. Biological Results

The novel 8-methyl-4-oxo-1,4-dihydroquinoline-3-carbohydrazide derivatives featuring various substituted benzoyl and N-phenyl carboxamide or carbothioamide moieties were synthesized and evaluated for their potential to prevent single-cycle replicable (SCR) HIV-1 (NL4-3) replication in HeLa cell culture. In addition, the cytotoxicity of the compounds was controlled to ensure that the anti-HIV activity was entirely free of cytotoxic activity. Zidovudine (AZT) was used as a positive control. Figure 4 summarizes the biological data of the synthesized compounds reported as EC₅₀ and CC₅₀.

All tested compounds exhibited CC₅₀ > 500 μ M, suggesting no significant cytotoxicity and a good safety profile according to the biological results. The antiviral activity profile of the compounds demonstrated that the synthesized compounds displayed antiviral activity with EC₅₀ values ranging from 75 to 150 μ M, which were lower than the reference drug. Compounds 8a-g possessing substituted benzoyl moieties were more active than compounds 9a-c and 10a-f containing N-phenyl carboxamide or carbothioamide groups. It can be concluded that the elongation of the linker decreased the anti-HIV activity. As shown in Figure 4, the variation of the substituents on the phenyl ring of compounds 8a-g, 9a-c, and 10a-f influenced the anti-HIV activity in the following order: F > Me > OMe > Cl > H. In addition, in compounds 8a-g, the position of substituents on the benzoyl ring affected the potency of compounds, as flour and methyl groups at the para-position showed slightly better activity than the meta-position. This agrees with the SAR of HIV IN inhibitors that generally contain flour groups on the hydrophobic portion. The best anti-HIV activity was observed for compound 8b containing 4-flourobenzoyl moiety with an EC₅₀ of 75 μ M.

3.3. Molecular Docking Study

Docking tests were carried out on the integrase active site to determine how the compounds under study may in-

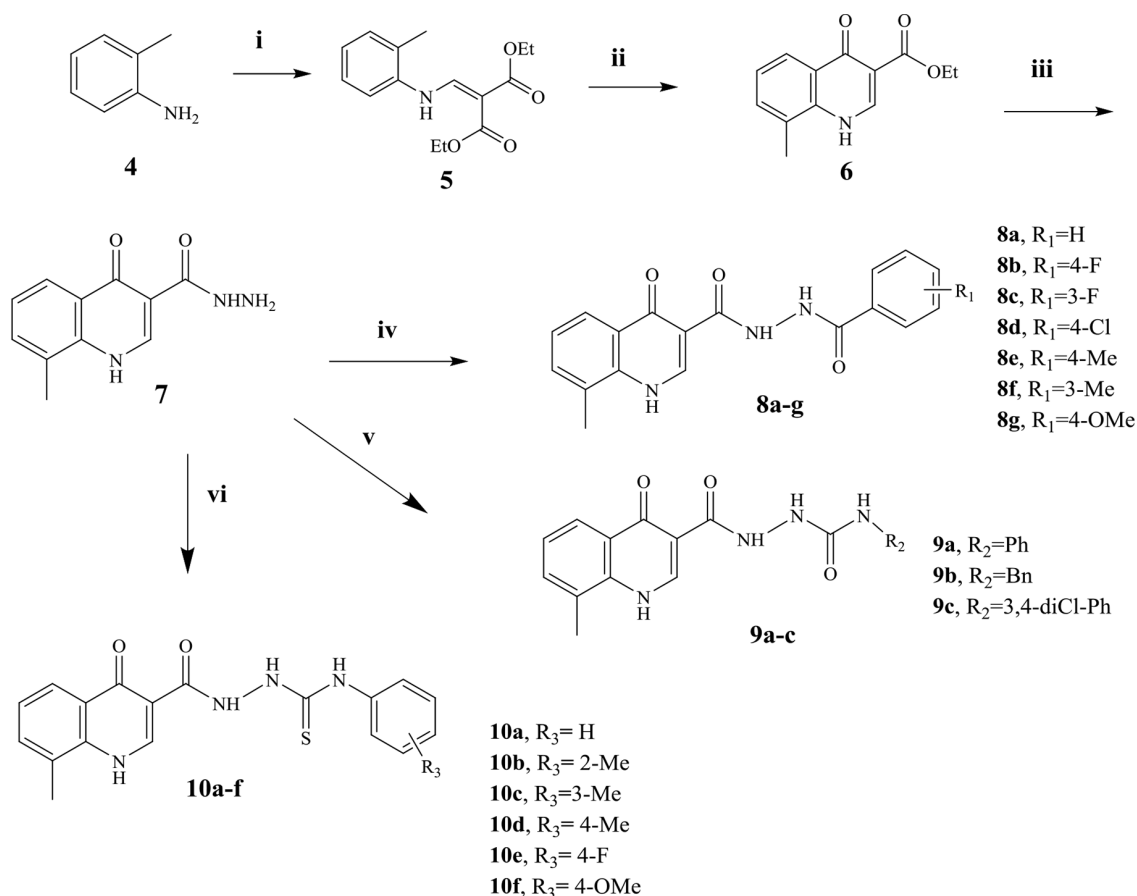


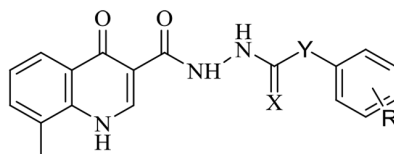
Figure 3. Reagents and conditions: (i) EMME, 125°C, 90 min; (ii) 2-chlorobenzoic acid, Ph₂O, 250°C, 120 min; (iii) NH₂NH₂, DMF, rt; (iv) benzoyl chloride derivatives, Na₂CO₃, DMF, rt, 17 h; (v) phenyl isocyanate derivatives, dry DMF, rt, 4 h; (vi) phenyl isothiocyanate derivatives, dry DMF, rt, 24 h

teract. The binding mode of substances in the IN active site was studied using compound 8b. AutoDock4 was used for the docking study, while PyMOL software was used to visualize and analyze the results. For docking studies, we utilized the PFV-IN structure in a complex with two magnesium ions (Mg²⁺), raltegravir, and a double-stranded DNA (DS) (PDB code: 3OYA). It has been previously reported that the PFV-integrase and HIV integrase secondary structures have a high degree of homology with an RMSD of 1.04 (39). The co-crystallized ligand, raltegravir, was redocked to verify the method. To calculate RMSD, we used the PyMOL program to superimpose the optimal pose on the co-crystallized raltegravir. As shown in Figure 4, the designed compounds exhibited good binding energy ranging from -6.93 to -8.15 kcal/mol. Compound 8b fitted well in the active site, indicating possible interactions with Mg²⁺ via its carbonyl moieties (Figure 5). In the hydrophobic pocket, the benzoyl ring interacted with the 3'-end-DAI7

through the π - π interactions. The flour group in the para position also could form hydrogen bonds at the active site (Figure 5). Overall, ligand 8b closely mimicked raltegravir's binding mode, as seen by a 3-D superposition of the two substances (Figure 6). According to docking studies, our molecules included the significant integrase pharmacophores inhibitors and may act via HIV integrase inhibition.

4. Conclusions

The research focused on the design and synthesis of 8-methyl-4-oxo-1,4-dihydroquinoline-3-carbohydrazide derivatives characterized by various substituted benzoyl and N-phenyl carboxamide or carbothioamide moieties based on the essential pharmacophores of HIV IN inhibitors. The in vitro anti-HIV and cytotoxicity assays of the proposed compounds exhibited that they were active



Compound	X	Y	R	EC ₅₀ (μM)	CC ₅₀ (μM)	Binding energy (kcal/mol)
8a	O	-	-H	140	> 500	-7.47
8b	O	-	4-F	75	> 500	-8.10
8c	O	-	3-F	80	> 500	-8.15
8d	O	-	4-Cl	110	> 500	-7.60
8e	O	-	4-Me	85	> 500	-7.70
8f	O	-	3-Me	88	> 500	-7.85
8g	O	-	4-OMe	100	> 500	-7.52
9a	O	-NH	-H	145	> 500	-7.28
9b	O	-NH-CH ₂	-H	N.D	> 500	-6.93
9c	O	-NH	3,4-Cl	N.D	> 500	-7.55
10a	S	-NH	-H	150	> 500	-7.20
10b	S	-NH	2-Me	N.D	> 500	-7.28
10c	S	-NH	3-Me	105	> 500	-7.37
10d	S	-NH	4-Me	100	> 500	-7.33
10e	S	-NH	4-F	90	> 500	-7.78
10f	S	-NH	4-OMe	N.D	> 500	-7.87
AZT		-	-	0.9	> 500	-

Figure 4. Anti-HIV activity, cytotoxicity, and binding energy of compounds 8a-g, 9a-c, and 10a-f

against HIV replication with EC₅₀ values ranging from 75 to 150 μM and CC₅₀ > 500 μM. The docking analysis demonstrated that the suggested compounds could interact with two Mg²⁺ ions and other critical residues in the active site of IN. Based on the low cytotoxicity and good anti-HIV activity, the 8-methyl-4-oxo-1,4-dihydroquinoline-3-carbohydrazide scaffold can be used for further development.

Footnotes

Authors' Contribution: Study concept and design: M. A.; analysis and interpretation of data: F. K. and R. V.; drafting of the manuscript: Z. H.; critical revision of the manuscript for important intellectual content: A. Z.

Conflict of Interests: The authors have no conflict of interest to declare.

Data Reproducibility: The data presented in this study are uploaded during submission as a supplementary file and are openly available for readers upon request.

Ethical Approval: This study was approved by the Ethics Committee of Shahid Beheshti University of Medical Sciences (SBMU), Iran, with approval number IR.SBMU.PHARMACY.REC.1399.343

Funding/Support: Research reported in this publication was supported by the Elite Researcher Grant Committee under award number 4002351 from the National Institute for Medical Research Development (NIMAD), Tehran, Iran.

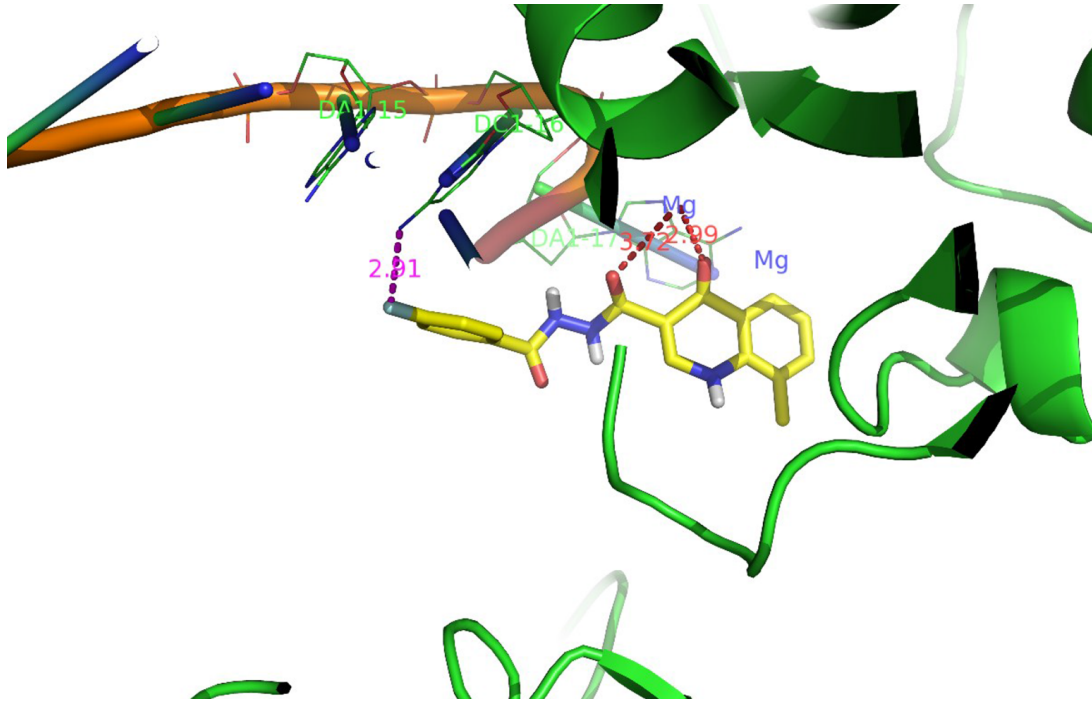


Figure 5. Compound 8b binding mode at the PFV IN active site (shown in yellow) (PDB 3OYA)

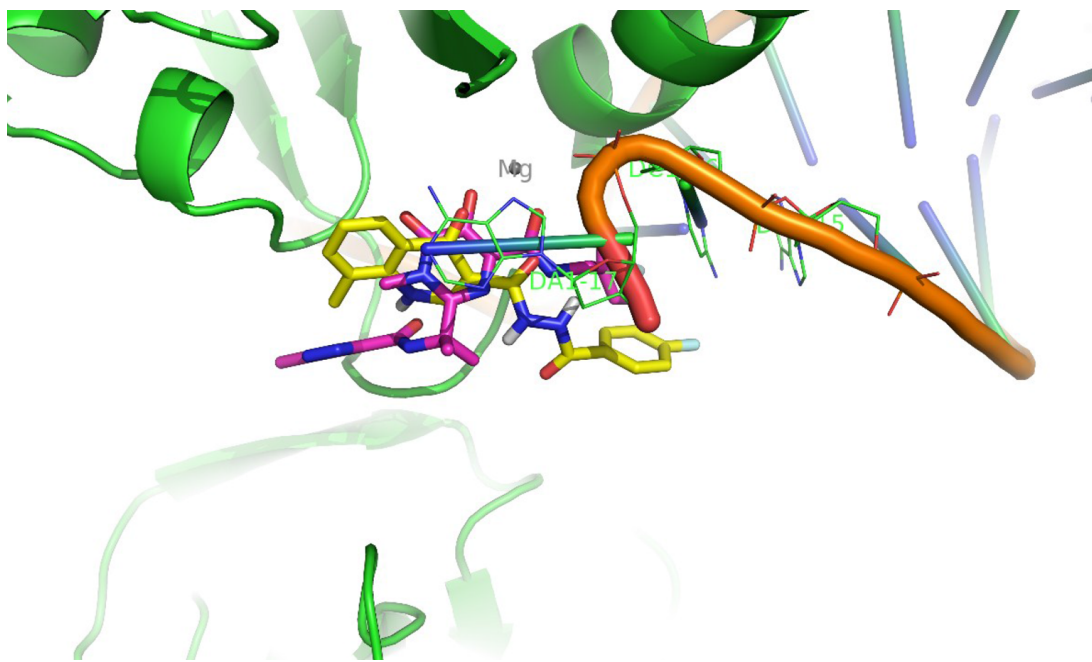


Figure 6. Compound 8b (shown in yellow) is superimposed over co-crystallized raltegravir (shown in purple) in the PFV IN active site

References

1. CDC. *Pneumocystis pneumonia—Los Angeles*. MMWR Morb Mortal Wkly Rep; 1981. Available from: <https://www.cdc.gov/mmwr/preview/mmwrhtml/lmrk077.htm>.
2. De Cock KM, Jaffe HW, Curran JW. Reflections on 40 Years of AIDS. *Emerg Infect Dis*. 2021;27(6):1553–60. doi: 10.3201/eid2706.210284. [PubMed: 34013858]. [PubMed Central: PMC8153860].
3. WHO. *HIV/AIDS*. 2017. Available from: <https://www.who.int/news-room/fact-sheets/detail/hiv-aids>.
4. Deeks SG, Overbaugh J, Phillips A, Buchbinder S. HIV infection. *Nat Rev Dis Primers*. 2015;1:15035. doi: 10.1038/nrdp.2015.35. [PubMed: 27188527].
5. Minwagaw MT, Akenie BB, Tewabe DS, Tegegne AS, Beyene TB. Predictors of Poor Adherence to CART and Treatment Failure at Second-Line Regimens Among Adults in Public Hospitals of Amhara Region, North-Western Ethiopia: A Retrospective Cohort Study. *Patient Prefer Adherence*. 2021;15:2855–64. doi: 10.2147/PPA.S339108. [PubMed: 34992354]. [PubMed Central: PMC8713999].
6. Caputo A, Gavioli R, Bellino S, Longo O, Tripiciano A, Francavilla V, et al. HIV-1 Tat-based vaccines: an overview and perspectives in the field of HIV/AIDS vaccine development. *Int Rev Immunol*. 2009;28(5):285–334. doi: 10.1080/08830180903013026. [PubMed: 19811313].
7. Larijani MS, Ramezani A, Sadat SM. Updated Studies on the Development of HIV Therapeutic Vaccine. *Curr HIV Res*. 2019;17(2):75–84. doi: 10.2174/1570162X17666190618160608. [PubMed: 31210114].
8. Huang YS, Yang JJ, Lee NY, Chen GJ, Ko WC, Sun HY, et al. Treatment of *Pneumocystis jirovecii* pneumonia in HIV-infected patients: a review. *Expert Rev Anti Infect Ther*. 2017;15(9):873–92. doi: 10.1080/14787210.2017.1364991. [PubMed: 28782390].
9. Weichseldorfer M, Afram Y, Heredia A, Rikhtegaran-Tehrani Z, Sajadi MM, Williams SP, et al. Combined cART including Tenofovir Disoproxil, Emtricitabine, and Dolutegravir has potent therapeutic effects in HIV-1 infected humanized mice. *J Transl Med*. 2021;19(1):453. doi: 10.1186/s12967-021-03120-w. [PubMed: 34717655]. [PubMed Central: PMC8557591].
10. Wang Z, Vince R. Synthesis of pyrimidine and quinolone conjugates as a scaffold for dual inhibitors of HIV reverse transcriptase and integrase. *Bioorg Med Chem Lett*. 2008;18(4):1293–6. doi: 10.1016/j.bmcl.2008.01.025. [PubMed: 18226894].
11. Cihlar T, Fordyce M. Current status and prospects of HIV treatment. *Curr Opin Virol*. 2016;18:50–6. doi: 10.1016/j.coviro.2016.03.004. [PubMed: 27023283].
12. Gordon CP, Griffith R, Keller PA. Control of HIV through the inhibition of HIV-1 integrase: a medicinal chemistry perspective. *Med Chem*. 2007;3(2):199–220. doi: 10.2174/157340607780059558. [PubMed: 17348857].
13. Wang JY, Ling H, Yang W, Craigie R. Structure of a two-domain fragment of HIV-1 integrase: implications for domain organization in the intact protein. *EMBO J*. 2001;20(24):7333–43. doi: 10.1093/emboj/20.24.7333. [PubMed: 11743009]. [PubMed Central: PMC125787].
14. Sayasith K, Sauve G, Yelle J. Targeting HIV-1 integrase. *Expert Opin Ther Targets*. 2001;5(4):443–64. doi: 10.1517/14728222.5.4.443. [PubMed: 12540259].
15. Isaacs D, Mikasi SG, Obasa AE, Ikomey GM, Shityakov S, Cloete R, et al. Structural Comparison of Diverse HIV-1 Subtypes using Molecular Modelling and Docking Analyses of Integrase Inhibitors. *Viruses*. 2020;12(9). doi: 10.3390/v12090936. [PubMed: 32858802]. [PubMed Central: PMC7552036].
16. Skinner LM, Sudol M, Harper AL, Katzman M. Nucleophile selection for the endonuclease activities of human, ovine, and avian retroviral integrases. *J Biol Chem*. 2001;276(1):114–24. doi: 10.1074/jbc.M007032200. [PubMed: 11024025].
17. Hare S, Maertens GN, Cherepanov P. 3'-processing and strand transfer catalysed by retroviral integrase in crystallo. *EMBO J*. 2012;31(13):3020–8. doi: 10.1038/emboj.2012.118. [PubMed: 22580823]. [PubMed Central: PMC3395085].
18. Goldgur Y, Dyda F, Hickman AB, Jenkins TM, Craigie R, Davies DR. Three new structures of the core domain of HIV-1 integrase: an active site that binds magnesium. *Proc Natl Acad Sci U S A*. 1998;95(16):9150–4. doi: 10.1073/pnas.95.16.9150. [PubMed: 9689049]. [PubMed Central: PMC21307].
19. Hajimahdi Z, Zarghi A. Progress in HIV-1 Integrase Inhibitors: A Review of their Chemical Structure Diversity. *Iran J Pharm Res*. 2016;15(4):595–628. [PubMed: 28243261]. [PubMed Central: PMC5316242].
20. Zeuli J, Rizza S, Bhatia R, Temesgen Z. Bictegravir, a novel integrase inhibitor for the treatment of HIV infection. *Drugs Today (Barc)*. 2019;55(11):669–82. doi: 10.1358/dot.2019.55.11.3068796. [PubMed: 31840682].
21. Rathbun RC, Lockhart SM, Miller MM, Liedtke MD. Dolutegravir, a second-generation integrase inhibitor for the treatment of HIV-1 infection. *Ann Pharmacother*. 2014;48(3):395–403. doi: 10.1177/1060028013513558. [PubMed: 24259658].
22. Shimura K, Kodama EN. Elvitegravir: a new HIV integrase inhibitor. *Antivir Chem Chemother*. 2009;20(2):79–85. doi: 10.3851/IMP1397. [PubMed: 19843978].
23. Cocohoba J, Dong BJ. Raltegravir: the first HIV integrase inhibitor. *Clin Ther*. 2008;30(10):1747–65. doi: 10.1016/j.clinthera.2008.10.012. [PubMed: 19014832].
24. Kovac L, Casar Z. A literature review of the patent application publications on cabotegravir - an HIV integrase strand transfer inhibitor. *Expert Opin Ther Pat*. 2020;30(3):195–208. doi: 10.1080/13543776.2020.1717470. [PubMed: 31944142].
25. Neamati N, Hong H, Owen JM, Sunder S, Winslow HE, Christensen JL, et al. Salicylhydrazine-containing inhibitors of HIV-1 integrase: implication for a selective chelation in the integrase active site. *J Med Chem*. 1998;41(17):3202–9. doi: 10.1021/jm9801760. [PubMed: 9703465].
26. Zhao H, Neamati N, Sunder S, Hong H, Wang S, Milne GW, et al. Hydrazide-containing inhibitors of HIV-1 integrase. *J Med Chem*. 1997;40(6):937–41. doi: 10.1021/jm960755+. [PubMed: 9083482].
27. Mouscadet JF, Desmaele D. Chemistry and structure-activity relationship of the styrylquinoline-type HIV integrase inhibitors. *Molecules*. 2010;15(5):3048–78. doi: 10.3390/molecules15053048. [PubMed: 20657464]. [PubMed Central: PMC6263292].
28. Batalha PN, da SL, Tolentino NMC, Sagrillo FS, de Oliveira VG, de Souza M, et al. 4-Oxoquinoline Derivatives as Antivirals: A Ten Years Overview. *Curr Top Med Chem*. 2020;20(3):244–55. doi: 10.2174/156802662066200129100219. [PubMed: 31995008].
29. Liu H, Duan Y, Xiong H, Zhang J, Huang S, Chen T, et al. Discovery of novel pyrrolo[2,3-b]pyridine derivatives bearing 4-oxoquinoline moiety as potential antitumor inhibitor. *Bioorg Med Chem Lett*. 2020;30(2):126848. doi: 10.1016/j.bmcl.2019.126848. [PubMed: 31836443].
30. Zhu J, He L, Ma L, Wei Z, He J, Yang Z, et al. Synthesis and biological evaluation of 4-oxoquinoline-3-carboxamides derivatives as potent anti-fibrosis agents. *Bioorg Med Chem Lett*. 2014;24(24):5666–70. doi: 10.1016/j.bmcl.2014.10.071. [PubMed: 25467157].
31. Fathy U, Gouhar RS, Younis A, El-Ghony DH. Synthesis of Novel pyrimido[4,5-b]quinoline-4-one Derivatives and Assessment as Antimicrobial and Antioxidant Agents. *Pharmacogn J*. 2020;13(2):550–62. doi: 10.5530/pj.2021.13.69.
32. Hajimahdi Z, Zabihollahi R, Aghasadeghi MR, Zarghi A. Design, synthesis and docking studies of new 4-hydroxyquinoline-3-carbohydrazide derivatives as anti-HIV-1 agents. *Drug Res (Stuttg)*. 2013;63(4):192–7. doi: 10.1055/s-0033-1334964. [PubMed: 23487403].
33. Hajimahdi Z, Zabihollahi R, Aghasadeghi MR, Ashtiani S, Zarghi A. Novel quinolone-3-carboxylic acid derivatives as anti-HIV-1 agents: design, synthesis, and biological activities. *Med Chem Res*. 2016;25(9):1861–76. doi: 10.1007/s00044-016-1631-x.
34. Morris GM, Huey R, Lindstrom W, Sanner MF, Belew RK, Goodsell DS, et al. AutoDock4 and AutoDockTools4: Automated docking

- with selective receptor flexibility. *J Comput Chem.* 2009;**30**(16):2785-91. doi: [10.1002/jcc.21256](https://doi.org/10.1002/jcc.21256). [PubMed: [19399780](https://pubmed.ncbi.nlm.nih.gov/19399780/)]. [PubMed Central: [PMC2760638](https://pubmed.ncbi.nlm.nih.gov/PMC2760638/)].
35. Lin CC, Cheng HY, Yang CM, Lin TC. Antioxidant and antiviral activities of *Euphorbia thymifolia* L. *J Biomed Sci.* 2002;**9**(6 Pt 2):656-64. doi: [10.1159/000067281](https://doi.org/10.1159/000067281). [PubMed: [12432232](https://pubmed.ncbi.nlm.nih.gov/12432232/)].
36. Scudiero DA, Shoemaker RH, Paull KD, Monks A, Tierney S, Nofziger TH, et al. Evaluation of a soluble tetrazolium/formazan assay for cell growth and drug sensitivity in culture using human and other tumor cell lines. *Cancer Res.* 1988;**48**(17):4827-33. [PubMed: [3409223](https://pubmed.ncbi.nlm.nih.gov/3409223/)].
37. Ebrahimzadeh E, Tabatabai SA, Vahabpour R, Hajimahdi Z, Zarghi A. Design, Synthesis, Molecular Modeling Study and Biological Evaluation of New N'-Arylidene-pyrido [2,3-d]pyrimidine-5-carbohydrazide Derivatives as Anti-HIV-1 Agents. *Iran J Pharm Res.* 2019;**18**(Suppl1):237-48. doi: [10.22037/ijpr.2019.112198.13597](https://doi.org/10.22037/ijpr.2019.112198.13597). [PubMed: [32802103](https://pubmed.ncbi.nlm.nih.gov/32802103/)]. [PubMed Central: [PMC7393058](https://pubmed.ncbi.nlm.nih.gov/PMC7393058/)].
38. Karimi N, Vahabpour Roudsari R, Azami Movahed M, Hajimahdi Z, Zarghi A. 4-(1-Benzyl-1H-benzo[d]imidazol-2-yl)-4-oxo-2-butenoic Acid Derivatives: Design, Synthesis and Anti-HIV-1 Activity. *Iran J Pharm Res.* 2021;**20**(1):408-17. doi: [10.22037/ijpr.2020.114341.14803](https://doi.org/10.22037/ijpr.2020.114341.14803). [PubMed: [34400969](https://pubmed.ncbi.nlm.nih.gov/34400969/)]. [PubMed Central: [PMC8170749](https://pubmed.ncbi.nlm.nih.gov/PMC8170749/)].
39. Yu S, Sanchez TW, Liu Y, Yin Y, Neamati N, Zhao G. Design and synthesis of novel pyrimidone analogues as HIV-1 integrase inhibitors. *Bioorg Med Chem Lett.* 2013;**23**(22):6134-7. doi: [10.1016/j.bmcl.2013.09.018](https://doi.org/10.1016/j.bmcl.2013.09.018). [PubMed: [24084160](https://pubmed.ncbi.nlm.nih.gov/24084160/)].